

# Synthesis, structure, linear and third-order nonlinear optical behavior of *N*-(3-hydroxybenzalidene)4-bromoaniline

Aslı Karakaş<sup>a</sup>, Hüseyin Ünver<sup>b</sup>, Ayhan Elmali<sup>c,\*</sup>

<sup>a</sup> Department of Physics, Faculty of Arts and Sciences, Selçuk University, TR-42049 Campus, Konya, Turkey

<sup>b</sup> Department of Physics, Faculty of Sciences, Ankara University, Tandoğan, TR-06100 Ankara, Turkey

<sup>c</sup> Department of Engineering Physics, Faculty of Engineering, Ankara University, Tandoğan, TR-06100 Ankara, Turkey

Received 21 May 2007; received in revised form 17 July 2007; accepted 17 July 2007

Available online 2 August 2007

## Abstract

*N*-(3-Hydroxybenzalidene)4-bromoaniline has been synthesized. Its crystal structure has been determined by X-ray diffraction analysis. To investigate microscopic third-order nonlinear optical (NLO) behavior of the title compound, we have computed both dispersion-free (static) and also frequency-dependent (dynamic) linear polarizabilities ( $\alpha$ ) and second hyperpolarizabilities ( $\gamma$ ) at  $\lambda = 825$ – $1125$  nm and  $1050$ – $1600$  nm wavelength areas using time-dependent Hartree–Fock (TDHF) method. The one-photon absorption (OPA) characterization has been theoretically obtained by means of configuration interaction (CI) method. The maximum OPA wavelengths are estimated in the UV region to be shorter than  $450$  nm, showing good optical transparency to the visible light. According to *ab-initio* calculation results on (hyper)polarizabilities, the synthesized molecule exhibits second hyperpolarizabilities with non-zero values, and it might have microscopic third-order NLO behavior.

© 2007 Elsevier B.V. All rights reserved.

**Keywords:** One-photon absorption; Static second hyperpolarizability; Dynamic second hyperpolarizability; Time-dependent Hartree–Fock; Configuration interaction

## 1. Introduction

Nonlinear optical (NLO) materials have been extensively studied for many years [1–5]. The search of new materials which have NLO properties is an important research field [6]. Significant interest still exists in the design and development of materials exhibiting large second-order NLO response because of the potential application in telecommunications, optical computing and optical signal processing [7–10]. Actually, the third-order response governed by the second hyperpolarizability offers more varied and richer behavior than the second-order NLO process due to the higher dimensionality of the frequency space. In the light of wide applications of NLO effects, a large number of materials have been synthesized and their NLO properties have been explored using different techniques

like degenerate four-wave mixing, Z-scan and third-harmonic generation (THG). THG measurements are particularly interesting since they are strongly related to electronic processes. For the free molecule, accurately determined experimental dipole and quadrupole moments and the (hyper)polarizabilities are known and could be reproduced by *ab-initio* calculations, if reasonably high correlation levels and large basis sets have been used [11–13]. However, experimental determination of the corresponding effective properties in condensed phases is much more difficult and rests on a number of assumptions and approximations whose limitations are difficult to assess.

Due to their centrosymmetric structures, non-substituted or symmetrically substituted organic compounds have been basically studied as third-order NLO materials. One could expect that the title Schiff base compound based on a centrosymmetric structure (Fig. 1) may show third-order NLO behavior. Theoretical calculations offer a quick and inexpensive way of predicting the NLO responses of

\* Corresponding author. Tel.: +90 312 2126720; fax: +90 312 2126742.  
E-mail address: [elmali@eng.ankara.edu.tr](mailto:elmali@eng.ankara.edu.tr) (A. Elmali).

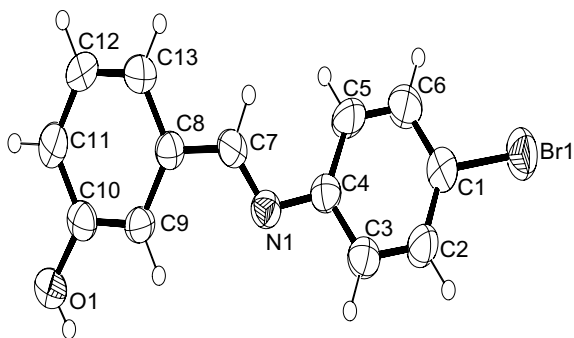


Fig. 1. The molecular structure of the title compound. Displacement ellipsoids are plotted at the 50% probability level and H atoms are presented as spheres of arbitrary radii.

the materials especially during the design of the new materials. Therefore, the present paper aims to give a contribution to the knowledge of the third-order optical nonlinearity of the synthesized and characterized (X-ray structure determination) title molecule by computing the maximum one-photon absorption (OPA) wavelengths and (hyper)polarizabilities with configuration interaction (CI) and *ab-initio* time-dependent Hartree–Fock (TDHF) methods.

## 2. Experimental

### 2.1. Preparation of *N*-(3-hydroxybenzalidene)4-bromoaniline

The title compound was prepared by the addition of 0.01 mol of 4-bromo-aniline in 60 ml of hot ethanol to 0.01 mol of 3-hydroxy-benzaldehyde in 80 ml of boiling ethanol, followed by heating to reflux for 4 h. Yellow crystals, suitable for X-ray analysis, were formed during reflux; found: C, 56.40%; H, 3.33%; N, 4.94%.  $C_{13}H_{10}BrNO$ : C, 56.55%; H, 3.65%; N, 5.07%.

### 2.2. X-ray structure determination

A suitable sample of size, for the title compound,  $0.06 \times 0.16 \times 0.44$  mm was chosen for the crystallographic study and then carefully mounted on goniometer of a STOE IPDS 2 diffractometer. All diffraction measurements were performed at room temperature (296 K) using graphite monochromated Mo-K $\alpha$  radiation. The intensities collected were corrected for Lorentz and polarization factors, absorption correction ( $\mu = 3.49$  mm $^{-1}$ ) by integration method via X-RED software [14] and cell parameters were determined by using X-AREA software [14]. The structure was solved by using direct methods in WINGX's implementation of SHELXS 97 [15]. The refinement was carried out by full-matrix least-squares method on the positional and anisotropic temperature parameters of the non-hydrogen atoms. All hydrogen atoms were located geometrically and refined as riding with respective C–H distance of 0.93 Å corresponding to the aromatic C–H and O–H bonds. The

scattering factors were taken from SHELXL-97 [16]. Other details of the data collection conditions and parameters of refinement process are summarized in Table 1. Selected bond distances and angles are listed in Table 2. The molecular structure with the atom-numbering scheme is shown in Fig. 1 [17]. Crystallographic data (excluding structure factors) for the structure reported in this paper have been deposited with the Cambridge Crystallographic Data Centre as Supplementary Publication No. CCDC 647118 [18].

## 3. Theoretical calculations

The theoretical computations involve the determination of dispersion-free and frequency-dependent linear polariz-

Table 1  
Crystal data and structure refinement for the title compound

Compound	$C_{13}H_{10}BrNO$
Colour/shape	Yellow/rod
Formula weight	276.13
Crystal system	Monoclinic
Space group	$P2_1/n$
Unit cell dimensions	
<i>a</i>	15.015(2) Å
<i>b</i>	5.3174(4) Å, $\beta = 108.30(1)^\circ$
<i>c</i>	15.436(1) Å
Volume	1170.1(2) Å $^3$
<i>Z</i>	4
Density (calculated)	1.567 g cm $^{-3}$
Absorption coefficient	3.49 mm $^{-1}$
<i>F</i> (000)	552
Crystal size	0.44 × 0.16 × 0.06 mm $^3$
$\theta$ range for data collection	3.30–29.95°
Index ranges	–20 ≤ <i>h</i> ≤ 20; –7 ≤ <i>k</i> ≤ 4; –21 ≤ <i>l</i> ≤ 20
Reflections collected	7529
Independent reflections	3075
Reflections observed ( <i>I</i> > 2 $\sigma$ ( <i>I</i> ))	1830
Refinement method	Full-matrix least-squares on $F^2$
Data/restraints/parameters	3075/0/153
Goodness-of-fit on $F^2$	1.035
<i>R</i> indices [ <i>I</i> > 2 $\sigma$ ( <i>I</i> )]	$R_1 = 0.0519$ ; $wR_2 = 0.1051$
<i>R</i> indices (all data)	$R_1 = 0.1171$ ; $wR_2 = 0.1424$
$(\Delta\rho)_{\max}$ , $(\Delta\rho)_{\min}$	–0.596, 0.332 e Å $^{-3}$

Table 2  
Some selected bond distances (Å), bond angles (°) and torsion angles (°) for the title compound

Br1–C1	1.907(3)	N1–C7	1.276(4)
N1–C4	1.426(4)	C1–C2	1.375(4)
C7–N1–C4	118.2(3)	C2–C1–Br1	120.0(3)
C3–C4–N1	119.4(3)	C5–C4–N1	123.1(3)
C6–C1–Br1	119.4(3)	N1–C7–C8	126.0(3)
Br1–C1–C2–C3	–178.6(3)	C2–C3–C4–N1	176.8(3)
C7–N1–C4–C3	148.6(3)	C7–N1–C4–C5	–37.3(5)
N1–C4–C5–C6	–175.9(4)	Br1–C1–C6–C5	179.3(3)
C4–N1–C7–C8	172.8(3)	N1–C7–C8–C13	–169.5(3)

ability and second hyperpolarizability tensor components of the title compound using the following methods.

As the first step of static and dynamic (hyper)polarizability calculations, the geometries taken from the starting structures in Table 2 have been optimized in the *ab-initio* restricted Hartree–Fock level. The optimized structures have been used to compute the linear polarizabilities and third-order hyperpolarizabilities at  $\omega$  frequencies with a triple-zeta valence (code-named TZV) basis set, which is a kind of extended basis sets [19–21]. The basis set effects are important for the calculation of NLO properties. Besides, while one computes the NLO properties for fairly large systems, extended basis sets consisting of Gaussian-type functions are found to be especially important. Augmenting the basis set of elements with diffuse *s*, *p* and *d* functions in a proper way could provide the best compromise between speed and accuracy of the computation. TZV basis set due to Dunning [19], McLean and Chandler [20], Wachters [21] has some contractions in the examined compound: [5*s*1*p*/3*s*1*p*] for H; [10*s*6*p*/5*s*3*p*] for C, N, O; [14*s*11*p*5*d*/9*s*6*p*2*d*] for Br atoms. Contracted Gaussian basis sets of TZV quality are presented for Li to Kr, and then advantages and necessary modifications of them are discussed in literature [22]. In general, TZV basis sets could be especially preferred to perform some quantum mechanical calculations of the compounds using the *ab-initio* package GAMESS [23] at the Hartree–Fock level. So, it could be said that TZV basis set is rather enough to compute (hyper)polarizabilities of the title molecule.  $\alpha(0;0)$  and  $\gamma(0;0,0,0)$  at  $\omega = 0$ ;  $\alpha(-\omega; \omega)$  and  $\gamma(-3\omega; \omega, \omega, \omega)$  calculations at  $\omega = 0.05512, 0.04050, 0.04336, 0.02848$  atomic units (a.u.) (i.e., at  $\lambda = 825, 1125, 1050, 1600$  nm wavelengths), often used laser frequencies in THG measurements, have been carried out using the TDHF method implemented in the GAMESS program [23]. In these  $\gamma$  definitions above-mentioned; the first describes the static third-order hyperpolarizabilities and the second represents the hyperpolarizability for frequency tripling, called the THG process. All (hyper)polarizability calculations have been performed on a PC with an Intel Pentium IV operator, 512 MB RAM memory and 1.7 GHz frequency using Linux PC GAMESS version running under Linux 7.3 environment.

In this study, the average linear polarizability  $\langle\alpha\rangle$  and third-order hyperpolarizability  $\langle\gamma\rangle$  values have been calculated using the following expressions, respectively [24]:

$$\langle\alpha\rangle = (\alpha_{xx} + \alpha_{yy} + \alpha_{zz})/3 \quad (1)$$

$$\langle\gamma\rangle = (1/5)[\gamma_{xxxx} + \gamma_{yyyy} + \gamma_{zzzz}2(\gamma_{xyyy} + \gamma_{xxzz} + \gamma_{yyzz})]. \quad (2)$$

Since  $\alpha$  and  $\gamma$  values of GAMESS output are reported in a.u., the calculated  $\alpha$  and  $\gamma$  values have been converted into the electrostatic units (esu) (1 a.u.  $\alpha = 0.1482 \times 10^{-24}$  esu, 1 a.u.  $\gamma = 5.0367 \times 10^{-40}$  esu). To calculate all the (hyper) polarizabilities, the origin of the cartesian coordinate system ( $x, y, z$ ) = (0,0,0) has been chosen at own center of mass of the studied compound in Fig. 1.

Besides, the  $\pi \rightarrow \pi^*$  transition wavelengths ( $\lambda_{\max}$ ) of the lowest lying electronic transition and the oscillator

strengths ( $f$ ) of these transitions for the investigated molecule have been theoretically studied by electron excitation configuration interaction using the CIS/6-31G method in GAUSSIAN98W [25] on an Intel Pentium IV 1.7 GHz processor with 512 MB RAM and Microsoft windows as the operating system.

## 4. Results and discussion

### 4.1. Description of the crystal structure

Conjugated organic molecules containing both donor and acceptor groups are of great interest for molecular electronic devices. Second-order NLO organic materials, which contain stable molecules with large molecular hyperpolarizabilities in non-centrosymmetric packing, are of great interest for device applications [26], but according to a statistical study, an overwhelming majority of achiral molecules crystallize centrosymmetrically [27].

The title molecule is not planar. Schiff base moieties **A** [C7–C13, O1; planar with a maximum deviation of 0.021(1) Å for the C7 atom] and **B** [N1, C1–C6, Br1; planar with a maximum deviation of 0.043(1) Å for the N1 atom] are inclined at an angle of 29.2(1)° reflecting mainly the twist about C7–N1 [C8–C7–N1–C4 = 172.8(3)°].

The crystal structure is stabilized by intermolecular hydrogen bonding. Intermolecular hydrogen bonding occurs between O15–H15...N1 [2.825(4) Å] (symmetry code: 0.5 – *x*, *y* – 0.5, 0.5 – *z*) atoms of neighbouring molecules as seen (Fig. 2).

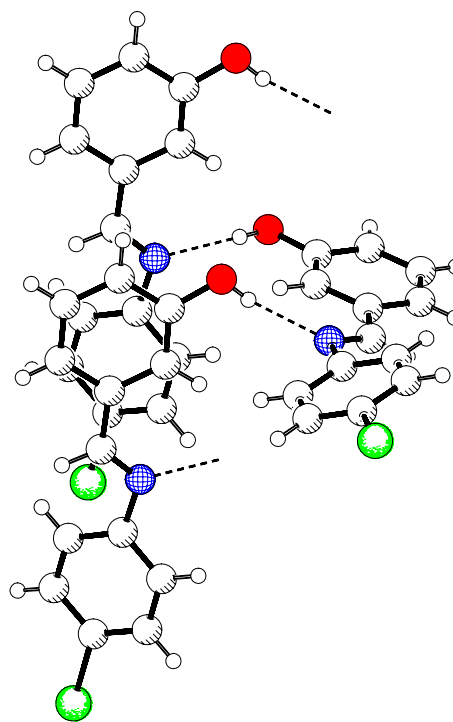


Fig. 2. A perspective view of the title molecule in the crystal structure. The intermolecular hydrogen bonds have been indicated by dashed lines.

Examination of the bond lengths suggests that there is an extended series of  $\pi$  bonds through the whole molecule. Except for the C7–N1 bond connecting and phenyl groups, all the other bonds between non-H atoms show  $\pi + \sigma$  character; the C–C bond lengths in the phenyl groups range from 1.355(6) to 1.409(4) Å. The C7–N1, C1–C2 and C5–C6 bond lengths are shorter than typical single  $\sigma$  bonds, and these bond lengths are in good agreement with related ligands in literature [28]. The Csp<sup>2</sup>–O bond associated with the oxygen atom is clearly a single bond, while the C7–N1 [1.276(4) Å] bond length shows a partial double bond character [28,29], which is also an evidence for the conjugation.

#### 4.2. Computational results and discussion

NLO techniques are considered as among the most structure-sensitive methods to study molecular structures and assemblies. Since the potential of organic materials for NLO devices have been proven, NLO properties of many of these compounds have been investigated by both experimental and theoretical methods [30]. In the past 5 years, the efforts on NLO have been largely devoted to preparing third-order NLO materials using theoretical methods and exploring the structure–property relationships. Quantum chemical calculations have been shown to be useful in the description of the relationship between the electronic structure of the systems and its NLO response [6]. The computational approach allows the determination of molecular NLO properties as an inexpensive way to design molecules by analyzing their potential before synthesis and to determine high-order hyperpolarizability tensors of molecules.

It can be very helpful in the investigation of NLO materials making it possible to check, apart from NLO responses, also spectroscopic absorbance in the appropriate wavelength. Thus, the wavelengths obtained by UV–vis spectral analysis can be helpful in planning the synthesis of the promising NLO materials only [31]. Since it is necessary to know the transparency region, the electronic absorption spectral studies of compounds designed to possess NLO properties are important. Albert et al. [32] have reached the conclusion that with the correct substitution of the push–pull system in the porphyrin ring, characterized by strong intramolecular  $\pi \rightarrow \pi^*$  charge transfer transitions found through UV–vis spectral analysis, some specific electronic and structural properties of this system could produce high NLO responses. Zhou et al. [33] have found that the  $\lambda_{\max}$  results of novel *para*-phenylenealkyne macrocycles are not accelerated with the odd number of unit, even with 10 units the value of  $\lambda_{\max}$  is 360 nm. Though the  $\lambda_{\max}$  was estimated to be shorter than 400 nm in an enough large sample, a strong increase in the hyperpolarizability value is obtained with a sizeable increase. Di Bella et al. [34] have reported that bis(salicylaldiminato) nickel(II) compound exhibited interesting linear optical features which will be seen to be related to the NLO response. There is a broad band in the region

between 300 and 360 nm involving mainly  $\pi \rightarrow \pi^*$  transitions. The band at around 400 nm is frequently suggestive of a large hyperpolarizability. In this paper, the vertical transition energies and oscillator strengths from the ground state to each excited state have been computed, giving OPA, i.e., the UV–vis spectrum. The calculated wavelengths ( $\lambda_{\max}$ ) and oscillator strengths ( $f$ ) for the maximum OPA of the investigated molecule are shown in Table 3. The molecule in Fig. 1 has four OPA peaks in its spectrum. As can be seen from Table 3, the optical spectra exhibit relatively intense four bands involving  $\pi \rightarrow \pi^*$  transitions centered between 220 and 405 nm. The values of all absorption maxima are located in the UV region estimated to be shorter than 450 nm, being transparent in the visible region.

Once conceived, the idea can be first pursued by theoretical means, and promising results would justify experimental efforts to obtain the envisioned compounds synthetically as well. One could determine the hyperpolarizability tensors of molecules using a suitable computational approach. These tensors describe the response of molecules to an external electric field. At the molecular level, the NLO properties are determined by their dynamic hyperpolarizabilities. TDHF is a procedure generally used to find out approximate values and can be a means of understanding both static and dynamic hyperpolarizabilities of organic molecules. We present here a comprehensive *ab-initio* study on the NLO properties of the title molecule using the TDHF method. In this study, in addition to the static linear polarizabilities  $\alpha(0;0)$  and second hyperpolarizabilities  $\gamma(0;0,0,0)$ , the following processes for dynamic (hyper)polarizabilities have been considered: frequency-dependent linear polarizabilities  $\alpha(-\omega;\omega)$ , THG  $\gamma(-3\omega;\omega,\omega,\omega)$ . Some significant calculated magnitudes of the static and frequency-dependent linear polarizabilities and second hyperpolarizabilities are shown in Tables 4–7, respectively.

The values of  $\gamma$  depend on the halogen substitution in the molecular structure. Further, the donor capacities of Br atoms are ordered in terms of their  $\sigma$  donation ability. So, one would expect the bromo compounds to exhibit lar-

Table 3

Calculated the maximum UV–vis absorption wavelengths ( $\lambda_{\max}$ , nm) and oscillator strengths ( $f$ ) of the title compound

$\lambda_{\max}$	$f$
405.32	2.0015
381.23	1.7366
249.46	1.4471
219.71	1.1269

Table 4

Some selected components of the static  $\alpha(0;0)$  and  $\langle\alpha\rangle(0;0)$  ( $\times 10^{-24}$  esu) value of the title compound

$\alpha_{xx}$	$\alpha_{yy}$	$\alpha_{zz}$	$\langle\alpha\rangle$
34.410	14.624	2.355	17.130

Table 5

Some selected components of the frequency-dependent  $\alpha(-\omega; \omega)$  and  $\langle\alpha\rangle(-\omega; \omega)$  ( $\times 10^{-24}$  esu) values at  $\omega$  (in a.u.) laser frequencies for the title compound

	$\omega = 0.05512$	$\omega = 0.04050$	$\omega = 0.04336$	$\omega = 0.02848$
$\alpha_{xx}$	33.165	32.596	32.692	32.258
$\alpha_{yy}$	14.818	14.725	14.741	14.671
$\alpha_{zz}$	2.304	2.294	2.295	2.287
$\langle\alpha\rangle$	16.762	16.538	16.576	16.406

Table 6

All static  $\gamma(0; 0, 0, 0)$  components and  $\langle\gamma\rangle(0; 0, 0, 0)$  ( $\times 10^{-37}$  esu) value for the title compound

$\gamma_{xxxx}$	$\gamma_{yyyy}$	$\gamma_{zzzz}$	$\gamma_{xxyy}$	$\gamma_{xxzz}$	$\gamma_{yyzz}$	$\langle\gamma\rangle$
970.455	4.471	0.752	-7.462	10.881	1.092	196.940

Table 7

Some selected components of the frequency-dependent  $\gamma(-3\omega; \omega, \omega, \omega)$  and  $\langle\gamma\rangle(-3\omega; \omega, \omega, \omega)$  ( $10^{-37}$  esu) values at  $\omega$  (in a.u.) laser frequencies calculated with THG process for the title compound

	$\omega = 0.05512$	$\omega = 0.04050$	$\omega = 0.04336$	$\omega = 0.02848$
$\gamma_{xxxx}$	3880.136	1876.169	2059.260	1587.109
$\gamma_{yyyy}$	6.586	5.397	5.585	4.804
$\gamma_{zzzz}$	0.027	-0.075	-0.0616	-0.077
$\gamma_{xxyy}$	-34.754	-13.445	-15.444	-8.635
$\gamma_{xxzz}$	10.067	7.435	7.439	11.046
$\gamma_{yyzz}$	1.462	1.249	1.279	1.166
$\langle\gamma\rangle$	777.417	375.830	412.592	318.292

ger second hyperpolarizabilities. The fact that we observe that  $\sigma$  donation may not be the only role on  $\gamma$  values for halogens. An alternative model to explain this trend is based on the  $\pi$  donation ability of halogen atom in the presence of  $\pi$  accepting ligands. In the Schiff bases, the valence orbitals of the nitrogen atom are the hybridized  $sp^2$ , with the orbitals of the non-bonding pair of electrons being coplanar with the bonding orbital [35]. This lone-pair orbital with a comparatively large electron density is markedly polar, and thus aids in the formation of intramolecular hydrogen bond between the *meta* hydroxyl group and nitrogen (O1–H...N1). The configuration of the orbitals and their electron density play an important role in strengthening the hydrogen bond. Also, the changes in the strength of the intramolecular hydrogen bonds are due to the transmission of inductive and resonance effects from the substituent group to the nitrogen orbital through a number of intermediate atoms. The effects of hydrogen bonds on optical properties of the crystal are important [36]. The magnitudes of static (hyper)polarizabilities are strongly enhanced by hydrogen bonds. The majority of molecular crystals with hydrogen bonding tend to enhance the NLO effects in the crystal structure [37]. So, the hydrogen bonds may be employed as NLO functional bonds in the material designing. With a great possibility the intramolecular hydrogen bond of the examined compound here affects non-zero  $\alpha$  and  $\gamma$  values in Tables 4–7. Besides, at the *meta* position, the NLO behavior is maximum for var-

ious substituents. The Schiff base system studied here has a donor hydroxy (–OH) group at the *meta* position. Therefore, it could be also said that this (–OH) group at the *meta* position of the investigated molecule may play important roles in determining its third-order optical nonlinearity.

## 5. Conclusions

The title compound has been synthesized for the study of its third-order optical nonlinearity. The structural characterization has been investigated by X-ray diffraction measurements. To understand the relationship between structure–property and NLO, we have extended our study to compute the OPA wavelengths, linear and second (hyper)polarizabilities using CI and TDHF methods. According to the calculation results on the linear optical behavior, the synthesized molecule is almost transparent in the visible and near-IR region (450–900 nm). It is especially essential to know theoretically the frequency-dependence of second hyperpolarizabilities at the laser frequencies often employed in the THG measurements. The *ab-initio* calculated non-zero (hyper)polarizability values imply that the examined compound might have microscopic third-order NLO behavior.

## Acknowledgement

This work was supported by Turkish State of Planning Organization (DPT), TÜBİTAK and Selçuk University under Grant Nos. 2003-K-12019010-7, 105T132, and 2003/030, respectively.

## References

- [1] A. Karakaş, A. Elmali, H. Ünver, H. Kara, Y. Yahsi, Z. Naturforsch. 61b (2006) 968.
- [2] H. Ünver, A. Elmali, A. Karakaş, H. Kara, E. Donmez, J. Mol. Struct. 800 (2006) 18.
- [3] K. Pedersen, T.G. Pedersen, T.B. Kristensen, P. Morgen, Appl. Phys. B 68 (1999) 637.
- [4] E.A. Perpète, J.M. André, B. Champagne, J. Chem. Phys. 109 (1998) 4624.
- [5] D.M. Bishop, J.M. Luis, B. Kirtman, J. Chem. Phys. 108 (1998) 10013.
- [6] D.M. Burland, R.D. Miller, C.A. Walsh, Chem. Rev. 94 (1994) 31.
- [7] T.G. Pedersen, K. Pedersen, P.K. Kristensen, J. Rafaelsen, N. Skivesen, Z. Li, S.V. Hoffmann, Surf. Sci. 516 (2002) 127.
- [8] A. Elmali, A. Karakaş, H. Ünver, Chem. Phys. 309 (2005) 251.
- [9] A. Karakaş, H. Ünver, A. Elmali, I. Svoboda, Z. Naturforsch. 60a (2005) 376.
- [10] A. Karakaş, A. Elmali, H. Ünver, I. Svoboda, J. Mol. Struct. 702 (2004) 103.
- [11] G. Maroulis, Chem. Phys. Lett. 289 (1998) 403.
- [12] E.R. Batista, S.S. Xantheas, H. Jónsson, J. Chem. Phys. 109 (1998) 4546.
- [13] O. Christiansen, J. Gauss, J.F. Stanton, Chem. Phys. Lett. 305 (1999) 147.
- [14] Stoe, Cie, X-AREA (version 1.18) and X-RED32 (version 1.04), Stoe & Cie, Darmstadt, Germany, 2002.
- [15] G.M. Sheldrick, SHELXS-97, Program for the Solution of Crystal Structures, University of Goettingen, Germany, 1997.

- [16] G.M. Sheldrick, SHELXL-97 Program for the refinement of Crystal Structures, University of Goettingen, Germany, 1997.
- [17] L.J. Farrugia, *J. Appl. Crystallogr.* 30 (1997) 565.
- [18] Further information may be obtained from: Cambridge Crystallographic Data Center (CCDC), 12 Union Road, Cambridge CB21EZ, UK, by quoting the Depository No. CCDC 266594, e-mail: deposit@ccdc.cam.ac.uk.
- [19] T.H. Dunning, *J. Chem. Phys.* 55 (1971) 716.
- [20] A.D. McLean, G.S. Chandler, *J. Chem. Phys.* 72 (1980) 5639.
- [21] A.J.H. Wachters, *J. Chem. Phys.* 52 (1970) 1033.
- [22] A. Schäfer, C. Huber, R. Ahlrichs, *J. Chem. Phys.* 100 (1994) 5829.
- [23] Intelx86 (win32, Linux, OS/2, DOS) version, PC GAMESS version 6.2, Build No. 2068. This version of GAMESS is described in: M.W. Schmidt, K.K. Baldridge, J.A. Boatz, S.T. Elbert, M.S. Gordon, J.H. Jensen, S. Koseki, N. Matsunaga, K.A. Nguyen, S.J. Su, T.L. Windus, M. Dupuis, J.A. Montgomery, *J. Comput. Chem.* 14 (1993) 1347.
- [24] (a) M.P. Bogaard, B. Orr, *J. Phys. Chem., Ser. 2*;  
(b) A.D. Buckingham (Ed.), *MTP International Review of Science*, vol. 2, Butterworths, London, 1975, p. 149.
- [25] M.J. Frisch, G.W. Trucks, H.B. Schlegel, G.E. Scuseria, M.A. Robb, J.R. Cheeseman, V.G. Zakrzewski, J.A. Montgomery, Jr., R.E. Stratmann, J.C. Burant, S. Dapprich, J.M. Millam, A.D. Daniels, K.N. Kudin, M.C. Strain, O. Farkas, J. Tomasi, V. Barone, M. Cossi, R. Cammi, B. Mennucci, C. Pomelli, C. Adamo, S. Clifford, J. Ochterski, G.A. Petersson, P.Y. Ayala, Q. Cui, K. Morokuma, D.K. Malick, A.D. Rabuck, K. Raghavachari, J.B. Foresman, J. Cioslowski, J.V. Ortiz, A.G. Baboul, B.B. Stefanov, G. Liu, A. Liashenko, P. Piskorz, I. Komaromi, R. Gomperts, R.L. Martin, D.J. Fox, T. Keith, M.A. Al-Laham, C.Y. Peng, A. Nanayakkara, C. Gonzalez, M. Challacombe, P.M.W. Gill, B. Johnson, W. Chen, M.W. Wong, J.L. Andres, C. Gonzalez, M. Head-Gordon, E.S. Replogle, J.A. Pople, GAUSSIAN98, Revision A.7, Gaussian Inc., Pittsburgh, PA, 1998.
- [26] C. Bosshard, K. Sutter, R. Schlessler, P. Günter, *J. Opt. Soc. Am. B10* (1993) 867.
- [27] J. Jacques, A. Collet, S.H. Willen, *Enantiomers, Racemates and Resolutions*, Wiley Interscience, New York, 1981.
- [28] Q. Yang, Y. Tang, W. Yang, H. Chen, *Acta Crystallogr. C54* (1998) 1532.
- [29] M.S. Wong, V. Gramlich, F. Pan, C. Bosshard, P. Günter, *Acta Crystallogr. C53* (1997) 757.
- [30] H.S. Nalwa, M. Hanack, G. Pawlowski, M.K. Engel, *Chem. Phys.* 245 (1999) 17.
- [31] J. Kulakowska, S. Kucharski, *Eur. Polym. J.* 36 (2000) 1805.
- [32] I.D.L. Albert, T.J. Marks, M.A. Ratner, *Chem. Mater.* 10 (1998) 753.
- [33] Y. Zhou, S. Feng, Z. Xie, *Opt. Mater.* 24 (2003) 667.
- [34] S. Di Bella, I. Fragala, I. Ledoux, M.A. Diaz-Garcia, P.G. Lacroix, T.J. Marks, *Chem. Mater.* 6 (1994) 881.
- [35] K. Bhat, K.J. Chang, M.D. Aggarwal, W.S. Wang, B.G. Penn, D.O. Frazier, *Mater. Chem. Phys.* 44 (1996) 261.
- [36] D. Xue, S. Zhang, *J. Phys. Chem. Solids* 57 (1996) 1321.
- [37] J. Zyss, J.F. Nicoud, M. Coquillay, *J. Chem. Phys.* 81 (1984) 4160.